International Journal of Heat and Mass Transfer 51 (2008) 5333–5343

Contents lists available at ScienceDirect

International Journal of Heat and Mass Transfer

journal homepage: www.elsevier.com/locate/ijhmt

Effect of an interfacial shear stress on steam condensation in the presence of a noncondensable gas in a vertical tube

Kwon-Yeong Lee, Moo Hwan Kim *

Mechanical Engineering Department, Pohang University of Science and Technology, San 31, Hyoja Dong, Pohang 790-784, Republic of Korea

ARTICLE INFO

Article history:
Received 22 June 2007
Received in revised form 8 February 2008
Available online 24 May 2008

Keywords:
Noncondensable gas
Condensation
Vertical tube
Interfacial shear stress

ABSTRACT

Experimental and analytical studies were performed to examine local condensation heat transfer coefficients in the presence of a noncondensable gas inside a vertical tube. The experimental data for pure steam and steam/nitrogen mixture bypass modes were compared to study the effects of noncondensable nitrogen gas on annular film condensation phenomena. The condenser tube had a relatively small inner diameter of 13 mm. The experimental results demonstrated that the local heat transfer coefficients increased as the inlet steam flow rate increased and the inlet nitrogen mass fraction decreased. The results obtained using steam/nitrogen mixtures with a low inlet nitrogen mass fraction were similar to those obtained using pure steam. Therefore, the effects of noncondensable gas on steam condensation were weak in the small-diameter condenser tube because of interfacial shear stress. A new correlation based on dimensionless shear stress and noncondensable gas mass fraction variables was developed to evaluate the condensation heat transfer coefficient inside a vertical tube with noncondensable gas, irrespective of the condenser tube diameter. A theoretical model using a heat and mass transfer analogy and simple models using four empirical correlations were developed and compared with the experimental data obtained under various experimental conditions. The predictions of the theoretical model and the simple model based on a new correlation were in good agreement with the experimental results.

1. Introduction

The System-integrated Modular Advanced ReacTor (SMART) is a small modular integral-type pressurized water reactor that is developed for the dual purposes of seawater desalination and small-scaled power generation. The reactor is designed for forced convection core cooling during start-up and normal operating conditions, and for natural circulation core cooling during an accident. SMART increases its degree of inherent safety using advanced designs, such as a passive residual heat removal system (PRHRS).

When an emergency such as the unavailability of feedwater or the loss of off-site power arises with SMART-P, the PRHRS passively removes the core decay heat via natural convection. The system is connected to the feedwater and steam pipes and consists of a heat exchanger submerged in a refueling water tank, a compensation tank, and check and isolation valves. The heat exchanger removes the heat from the reactor coolant system through a steam generator via condensation heat transfer to water in the refueling water tank. The compensating tank is pressurized using a nitrogen gas to make up the water volume change in the PRHRS. Before PRHRS operation, nitrogen may be dissolved in the cooling water of the PRHRS. Therefore, during PRHRS operation, nitrogen gas might be generated due to evaporation in the steam generator, which will act as a noncondensable gas in the condensation heat exchanger.

Even a small amount of noncondensable gas can reduce the condensation heat transfer considerably. In the condenser tube, the condensate flows as an annular liquid film adjacent to the tube wall, while the vapor/noncondensable gas mixture flows in the core region. Consequently, the noncondensable gas layer that forms adjacent to the liquid/gas interface reduces the heat transfer capability.

Recently, several experimental studies have investigated condensation in the presence of noncondensable gas in a vertical tube. Vierow and Schrock [1], Siddique et al. [2], Araki et al. [3], Kuhn et al. [4], and Park and No [5] performed steam condensation experiments in air or helium using the secondary jacket cooling method. Kim [6] and Oh and Revankar [7] conducted steam/air condensation experiments with secondary pool boiling. Table 1 summarizes previous steam condensation experiments in a vertical tube in the presence of noncondensable gases.

To calculate the local heat fluxes, Siddique et al. [2] measured the local coolant bulk temperatures at the midpoint of the annular gap between the condenser tube and cooling jacket. A small amount of air was injected through the annulus with the cooling water to enhance the turbulence and mixing. However, this two-phase flow pattern introduced uncertainty caused by local fluctuations in the local temperature measurements. Furthermore, to

* Corresponding author. Tel.: +82 54 279 2165; fax: +82 54 279 3199.
E-mail address: mhkim@postech.ac.kr (M.H. Kim).

0017-9310/$ - see front matter © 2008 Elsevier Ltd. All rights reserved.
doi:10.1016/j.ijheatmasstransfer.2008.03.017

Nomenclature

B_h	suction parameter
C_p	specific heat [J/kg K]
D	diffusion coefficient [m^2/s]
d	diameter [m]
f	degradation factor, fanning friction factor
G^∞	mixture mass flux [kg/m^2 s]
g	acceleration due to gravity [m/s^2]
h	heat transfer coefficient [W/m^2 K]
h_m	mass transfer coefficient [$mole/m^2$ s]
i_{fg}	latent heat of vaporization [J/kg]
Ja	Jakob number
k	thermal conductivity [W/m K]
L	characteristic length scale
$\dot{m}$	mass flow rate [kg/s]
m''_{cond}	interfacial mass flux [kg/m^2 s]
Nu	Nusselt number
P	pressure [k Pa]
Pr	Prandtl number
q''	heat flux [W/m^2]
Re	Reynolds number
Sc	Schmidt number
Sh	Sherwood number
St	Stanton number
T	temperature [°C]
W	noncondensable gas mass fraction
x	distance from tube inlet [m]

Greek symbols

Δ	change
δ	condensate film thickness [m]
δ^*	dimensionless film thickness
μ	dynamic viscosity [Ns/m^2]
ρ	density [kg/m^3]
τ	shear stress [N/m^2]
τ^*_g	dimensionless shear stress

Subscripts

b	bulk
c	latent (or condensation)
cw	cooling water
cond	condensate
exp	experiment
f	film
g	gas phase
i	inner, interface
in	inlet
l	liquid
mix	vapor/noncondensable mixture
N_2	nitrogen gas
nc	noncondensable gas
Nu	Nusselt's theory
o	outer, without suction
other	other effects
pure	pure steam
r	rough
s	steam, sensible, smooth
shear	shear effect
sus	304 stainless steel
t	developing
w	wall

achieve good mixing, the air flow rate had to be so high that transition from bubbly to slug flow could occur. Kuhn et al. [4] and Park and No [5] calculated the local coolant bulk temperatures numerically by measuring temperatures at the inner and outer walls of the annulus; however, this method required extra effort to perform the numerical calculations and the data reduction process was complicated. Araki et al. [3] and Kim [6] calculated local heat fluxes by measuring the temperature gradient of the tube wall, but their results had a large experimental error; a small error in the distance between the inner and outer wall thermocouple locations introduced a very large uncertainty to their heat flux calculations, as the distance was very short due to the small tube thickness.

Also, many numerical studies have examined condensation in a vertical tube in the presence of noncondensable gas. Either boundary layer analysis or the heat and mass transfer analogy is generally used to analyze the heat and mass transfer. In boundary layer analysis, the governing equations for the condensation process including the vapor/noncondensable gas mixture and liquid film regions are solved with an appropriate boundary layer approximation. The boundary layer solutions deal primarily with the flat plate configuration and stagnant atmospheric conditions. In the heat and mass transfer analogy models, the general methodology of Colburn and Hougen [8] gives the basic idea for solving the condensation of vapor with noncondensable gas. In their method, the main equation involves the heat balance at the liquid/gas interface between the heat transfer through the vapor/noncondensable gas boundary layer and that through the condensate film. The heat and mass analogy method deals primarily with the vertical tube configuration and forced convection conditions for simplicity and gives a relatively good prediction.

Wang and Tu [9] presented the first solution of the effects of a noncondensable gas on the film-wise condensation of a vapor/noncondensable gas mixture with turbulent flow in a vertical tube using the heat and mass transfer analogy. They found that the reduction in heat transfer due to the noncondensable gas was more significant at low pressures and mixtures with low Reynolds numbers. Kageyama et al. [10] presented the diffusion layer theory for turbulent vapor condensation with noncondensable gases using 'effective condensation thermal conductivity.' This simple parameter was derived by expressing the driving potential for mass transfer as the difference in saturation temperatures and using appropriate thermodynamic relationships. Siddique [11] conducted an analytical study using the analogy between heat and mass transfer. That model included the effects of developing flow, condensate film roughness, and property variation in the gas phase. Munoz-Cobo et al. [12] developed approximate methods to calculate the condensate film thickness without the need to solve the transcendental equation that depends on the film thickness iteratively. Then, they applied the diffusion layer theory in the gas phase to consider the presence of a noncondensable gas. No and Park [13] developed both iterative and non-iterative models for steam condensation with noncondensable gas in a vertical tube. The non-iterative condensation model was proposed for easy engineering application using the iterative condensation model and the assumption of the same profile of the steam mass fraction as that of gas temperature in the gas boundary layer. Maheshwari et al. [14] investigated condensation in presence of a noncondensable gas for a wide range of Reynolds number. Their model incorporated Nusselt equation with McAdams modifier and Blangetti model to calculate the film heat transfer coefficient, and Moody correlation

Table 1
Previous steam condensation experiments in a vertical tube with noncondensable gas

	Vierow and Schrock [1]	Siddique et al. [2]	Araki et al. [3]	Kuhn et al. [4]	Park and No [5]	Kim [6]	Oh and Revankar [7]	Lee and Kim
Tube length (m)	2.1	2.54	2.0	2.4	2.4	1.8	0.984	2.8
Tube ID (mm)	22	46	49.5	47.5	47.5	46.2	26.6	13
Thickness (mm)	1.65	2.4	5.5	1.65	1.65	2.3	3.38	2.5
Jacket ID (mm)	50.8	62.7	159.2	76.2	100	–	–	40
Noncondensable gas	Air	Air/Helium	Air	Air/Helium	Air	Air	Air	Nitrogen
Secondary cooling	Forced convection	Forced convection	Forced convection	Forced convection	Forced convection	Pool boiling	Pool boiling	Forced convection
Steam flow (kg/h)	5.9–24.95	7.9–31.9	9.0–58.0	28.3–61.9	7.6–40.0	–	9.0–19.8	6.5–28.2
Inlet NC gas mass fraction (%)	0–14	10–35	0–24	0–40	10–40	0–30	0–10	0–40
Pressure (MPa)	0.03–0.45	0.1–0.5	0.15–0.25	0.1–0.5	0.17–0.5	0.35–7.5	0.1–0.4	0.1–0.13
HTC(W/m^2 K)	0–16,000	100–25,000	–	500–13,000	100–7000	4000–7400	3500–6500	300–27,900

and Wallis correlation to account for film waviness effect on gas boundary layer. And then, a comparative study with various models was made. Oh and Revankar [15] developed an empiricism-free or minimum empirical mechanistic model. They used general momentum, heat, and mass transport relations derived using an analytic method, and considered the surface suction effect.

The main objective of the present study was to improve the design of a PRHRS condensation heat exchanger by investigating its heat transfer characteristics. Nitrogen acts as the noncondensable gas in this heat exchanger, but no data are available for steam condensation in the presence of nitrogen. The condenser tube diameter in a PRHRS heat exchanger is smaller than those studied in previous research (see Table 1). Therefore, a database was generated for the condensation heat transfer of pure steam and a steam/nitrogen mixture inside a small-diameter condenser tube. We also developed a theoretical model using a heat and mass transfer analogy and simple models using four empirical correlations to investigate the effects of air or nitrogen on the heat transfer coefficient of steam condensing inside a vertical tube.

2. Experiment

2.1. Experimental apparatus

A schematic of the experimental apparatus is shown in Fig. 1. The experimental facilities consisted of a steam generator, steam flow rate control system, steam/nitrogen gas mixing system, test section, and data acquisition system.

The steam came from a gasoline boiler controlled by an on/off operation at a gauge pressure of 3–5 kgf/cm^2. A surge tank was installed before the steam supply line to minimize the effect of pressure fluctuations in the boiler on the steam flow rate. A moisture separator was installed between the surge tank and the steam flow rate control system to supply pure steam with a 100% quality. A steam supply line with a 15-mm inner diameter (ID) was used to measure a steam flow rate of 5–30 kg/h. The steam supply line had a RTD and a pressure transducer to measure the temperature and pressure to calculate the density of the steam, and a vortex flow meter to measure the volumetric steam flow rate. The flow computer and flow controller were connected to a steam pneumatic control valve to obtain the desired steam mass flow rate. The steam/nitrogen gas mixing system consisted of a nitrogen gas mass flow rate controller, a pre-heater, a chamber, and several valves.

The test section consisted of an inner condenser tube and an outer cooling jacket, as shown in Fig. 2. The condenser tube was made from a 3-m-long, 304 stainless steel pipe with a 13-mm ID, 2.5 mm thickness, and 2.8-m effective length. Sheathed 0.01-in.-diameter K-type thermocouples (T/Cs) were silver-welded onto the outer surface of the condenser tube at 13 different axial locations, 0.05, 0.20, 0.35, 0.50, 0.70, 0.90, 1.15, 1.40, 1.65, 1.90, 2.15, 2.40, and 2.65 m from the start of the effective length to measure

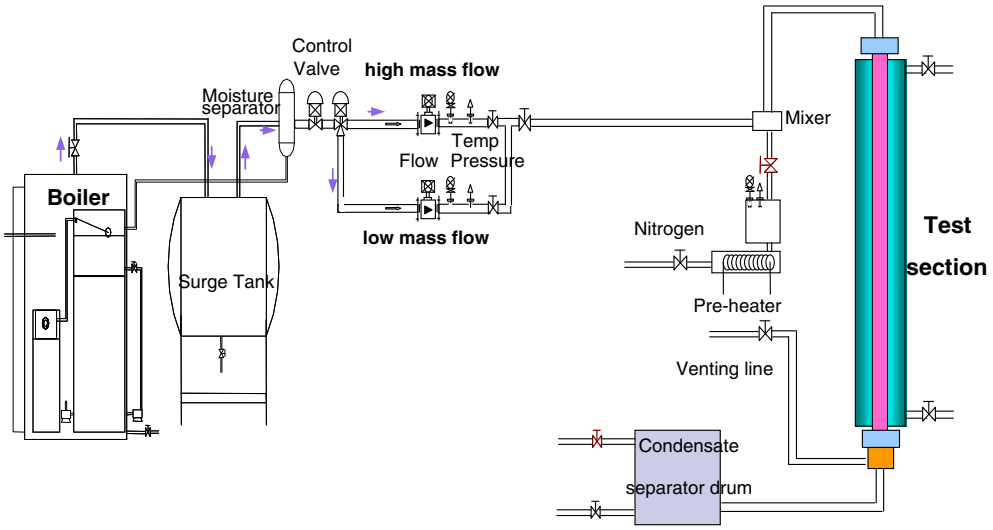

Fig. 1. Schematic diagram of the experimental apparatus.

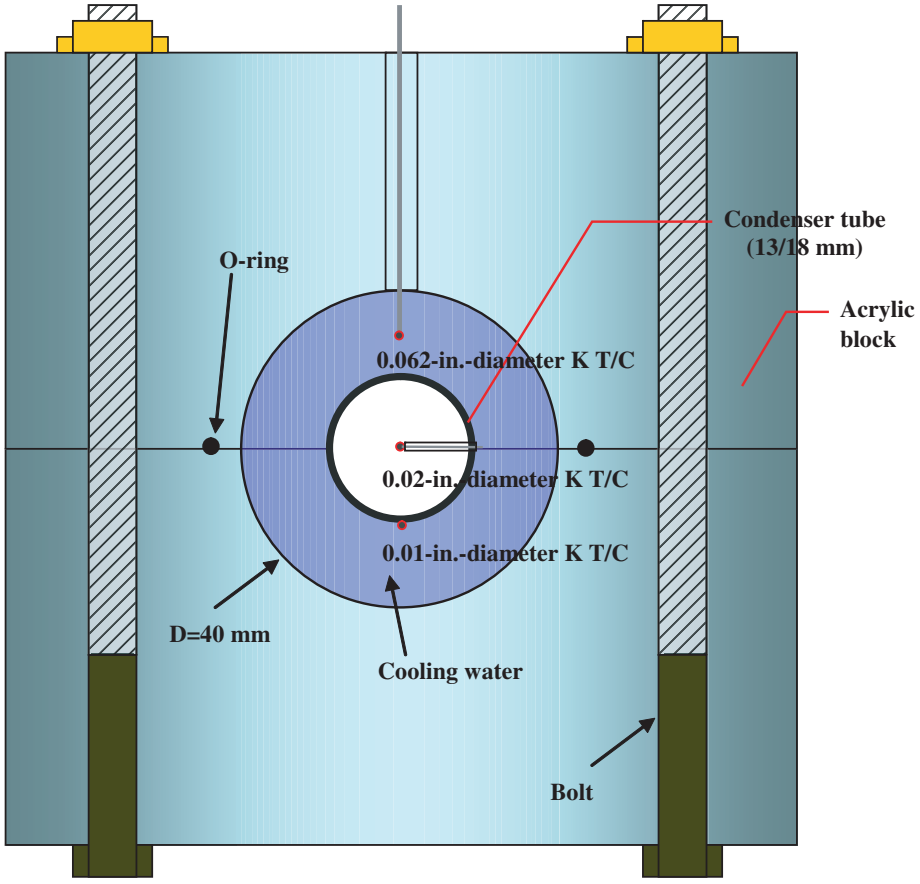

Fig. 2. Sheared view of condenser tube and cooling jacket.

the outer wall temperatures. At the same locations, 0.01-m-long stainless steel tubings were inserted through the condenser tube wall horizontally. Sheathed 0.02-in.-diameter K-type thermocouples were then inserted through those tubings and silver-welded onto the outer surface of the condenser tube to measure the centerline bulk temperatures. All of the wall and bulk thermocouple wires were taken out through the head of the cooling jacket. Two high-precision calibrated pressure transducers and one differential pressure transducer were used to measure the absolute pressures and the differential pressure between the entry and exit of the test section.

Three pairs of approximately 1-m-long acrylic blocks, for a total of six blocks, were installed around the condenser tube, forming an annulus for the cooling water flowing between the condenser tube and the acrylic blocks. The acrylic cooling jackets had a 40-mm ID. The local coolant bulk temperatures were measured at 11 different axial locations: the inlet, the outlet, and at 0.11, 0.45, 0.79, 1.09, 1.39, 1.69, 1.99, 2.33, and 2.67 m from the start of the effective length. Sheathed 0.062-in.-diameter rigid K-type thermocouples were inserted through the cooling jacket wall to the midpoint of the annular gap. Peterson et al. [16] identified the weak points of several different experimental techniques that had been used to determine the coolant bulk temperatures and the condensation heat fluxes. Even though the bubble mixing technique also has disadvantages as the temperature fluctuation and transition from bubble to slug flow, the local heat fluxes were calculated from the gradient of the measured coolant bulk temperatures when small amounts of air were bubbled through the annulus along with the cooling water for the reasons given by Siddique et al. [2] like the enhancement of turbulence and mixing in cooling water. At least one weak point of this technique was eliminated because the acrylic cooling jacket was transparent and the flow pattern inside the annulus was checked.

2.2. Data analysis

The present study only focused on the condensation phenomena, except for the single-phase region of the pure steam mode. Thus, the local heat flux could be obtained using the slope of the coolant temperature profile in the phase change region:

$$q''(x) = -\frac{\dot{m}_{cw} C_p}{\pi d_i} \frac{dT_{cw}(x)}{dx}. \tag{1}$$

The slope of the cooling water temperature profile was determined from a least-squares polynomial fit of the coolant temperatures as a function of the condenser length. The inner wall temperature was calculated using the measured outer wall temperature and the obtained heat flux:

$$T_{w,i}(x) = T_{w,o}(x) + q''(x) \cdot \frac{d_i \ln(d_o/d_i)}{2 \cdot k_{sus}}. \tag{2}$$

Then the local heat transfer coefficient was calculated using the heat flux, inner wall temperature, and bulk mixture temperature:

$$h(x) = \frac{q''(x)}{(T_b - T_{w,i})}. \tag{3}$$

The local condensate film flow rate was determined by integrating the heat balance equation between the heat flow rate and the latent heat transfer:

$$\dot{m}_{cond} = \pi d_i \int_0^x \frac{q''_j(x')}{i_{fg}(x')} dx'. \tag{4}$$

Here, the gas-phase sensible heat transfer was neglected.

The local steam flow rate was determined by subtracting the local condensate flow rate from the known inlet steam flow rate. Then the local nitrogen gas mass fraction was calculated using

$$W_{N_2}(x) = \frac{\dot{m}_{N_2}(x)}{\dot{m}_s(x) + \dot{m}_{N_2}(x)}. \quad (5)$$

Here, the nitrogen gas mass flow rate was assumed to be constant.

2.3. Experimental error

From Eqs. (1) and (3), the uncertainty associated with the heat transfer coefficient can be given by

$$\frac{\sigma_h}{h} = \left[\left(\frac{\sigma_{q''}}{q''}\right)^2 + \left(\frac{\sigma_{(T_b - T_{w,i})}}{(T_b - T_{w,i})}\right)^2\right]^{1/2} = \left[\left(\frac{\sigma_{\dot{m}_{cw}}}{\dot{m}_{cw}}\right)^2 + \left(\frac{\sigma_{(dT_{cw}/dL)}}{(dT_{cw}/dL)}\right)^2 + \left(\frac{\sigma_{(T_b - T_{w,i})}}{(T_b - T_{w,i})}\right)^2\right]^{1/2}. \quad (6)$$

Here, the K-type thermocouples were calibrated within a ±0.1 °C error limit. The turbine meter used to measure the flow rate of the cooling water had a ±0.5% accuracy. The variables C_p, d_o, and d_i were assumed to be error-free. The error associated with the local heat transfer at the first location, 0.05 m, was too large for the data to be meaningful and those data was not considered here.

In the pure steam test, the error increased from 6.8% to 57.0% as the inlet steam flow rate increased in the upper condenser tube. The large error was due to the relatively small temperature difference between the bulk and inner wall temperatures. In this paper, we only used data with an error less than 19.2% for pure steam test to analyze the condensation phenomena correctly.

In the mixture bypass test, the errors increased very rapidly downstream of the test section. In this region, the large nitrogen mass fraction acted as a large thermal resistance to the condensation heat transfer, reducing the heat flux. Eventually, the temperature gradient of the cooling water decreased and a large error was introduced. However, this large error region was not of interest because almost all of the condensation occurred within the first meter of the tube, which had lower uncertainties. In our analysis, we used data with an error less than 20.1% for mixture bypass test.

3. Experimental results

3.1. Results of condensation tests

The pure steam and steam/nitrogen mixture condensation tests were run at inlet steam flow rates of 6.5–28.2 kg/h with an inlet nitrogen mass fraction ranging from 0% to 40%. The operating pressure was close to atmospheric.

Fig. 3 shows that the local heat transfer coefficients increased as the inlet steam flow rate increased at the same inlet nitrogen mass fraction. Fig. 4 shows that the effect of the inlet noncondensable gas mass fraction on the condensation heat transfer coefficients at the same inlet steam flow rate. As the inlet noncondensable gas mass fraction increased, the local heat transfer coefficients decreased. In the present data obtained for a 13-mm-ID condenser tube, as shown in Fig. 4a, the local heat transfer coefficients were relatively small after a tube length of about 1 m. This indicates that the tube beyond a length of 1 m did not play an important role in the heat transfer, which should be considered when determining the thermal size of a PRHRS heat exchanger. The heat transfer coefficients of the steam/nitrogen mixture with a 3% inlet nitrogen mass fraction were almost the same as those of pure steam condensation. In previous research with relatively large-diameter

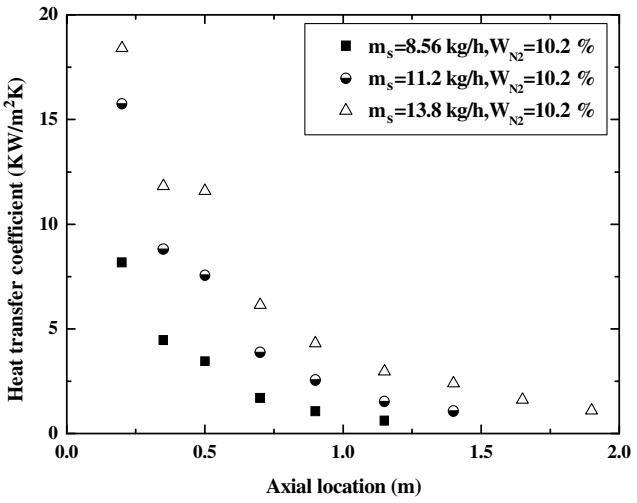

Fig. 3. Comparison of experimental heat transfer coefficients with the variation of the inlet steam flow rate.

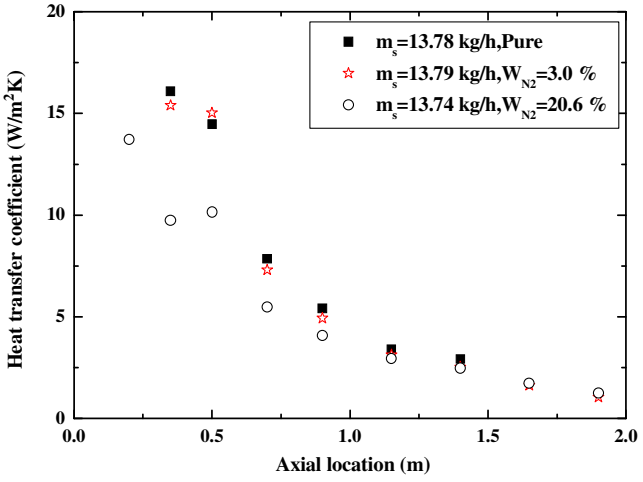

(a) Present data

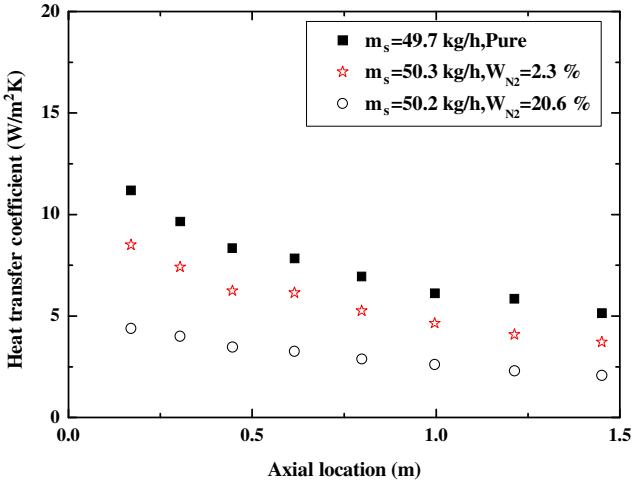

(b) Kuhn's data

Fig. 4. Comparison of experimental heat transfer coefficients with the variation of the inlet noncondensable gas mass fraction.

condenser tubes, however, the effect of the noncondensable gas was significant even when the inlet noncondensable gas mass fraction was very small. For example, the data of Kuhn [22] (shown in Fig. 4b) were obtained for a 47.5-mm-ID condenser tube with a similar Reynolds number and system pressure as the present data given in Fig. 4a, and the heat transfer coefficients of steam/air mixtures with very small air mass fractions differed from those of pure steam. Therefore, our results suggest that noncondensable gas has only a weak influence on steam condensation in small-diameter than large-diameter condenser tubes with the same inlet mixture Reynolds number.

3.2. Development of new empirical correlation

The interfacial shear stress increases as the condenser tube diameter decreases for the same mixture Reynolds number. The condensation heat transfer coefficients also increase due to the shear stress. The effect of the interfacial shear stress was not sufficiently considered in previous correlations using the Reynolds number. Thus the dimensionless shear stress τ^*_{mix} and noncondensable gas mass fraction W_{nc} were used to develop a new correlation. The degradation factor f defined as the ratio of the experimental heat transfer coefficient to a reference heat transfer coefficient was used to correlate the present data because of its simplicity.

Here, the dimensionless shear stress was defined as

$$\tau^*_{mix} = \frac{\tau_{mix}}{g\rho_f L} = \frac{1/2\rho_{mix}u^2_{mix}\cdot f}{g\rho_f L}, \tag{7}$$

where $u_{mix} = Re_{mix}\mu_{mix}/\rho_{mix}d_i$, $L = (\nu_f^2/g)^{1/3}$, and $f = 0.079Re_{mix}^{-1/4}$ for $Re_{mix} > 2300$ or $f = 16/Re_{mix}$ for $Re_{mix} < 2300$. The factor for the pure steam condensation heat transfer f_{pure} was correlated against the dimensionless shear stress of pure steam τ^*_{pure}, as shown in Fig. 5. This gives

$$f_{pure} = h_{exp,pure}/h_{Nu} = 0.8247\tau^{*0.3124}_{pure}. \tag{8}$$

The correlation for the effect of noncondensable gas was obtained by plotting the data set of mixture bypass mode in the form $(1 - f/\tau^{*0.3124}_{mix})$ versus W_{nc}, as shown in Fig. 6. Thus the final form of new correlation is given by

$$f = h_{exp,mix}/h_{Nu} = f_1 \cdot f_2 = \tau^{*0.3124}_{mix}(1 - 0.964W^{0.402}_{nc}) \tag{9}$$

for $0.06 < \tau^*_{mix} < 46.65$ and $0.038 < W_{nc} < 0.814$.

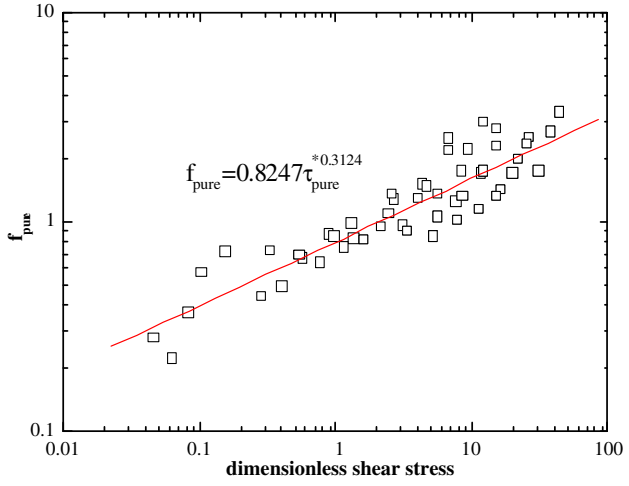

Fig. 5. Factor for pure steam condensation heat transfer.

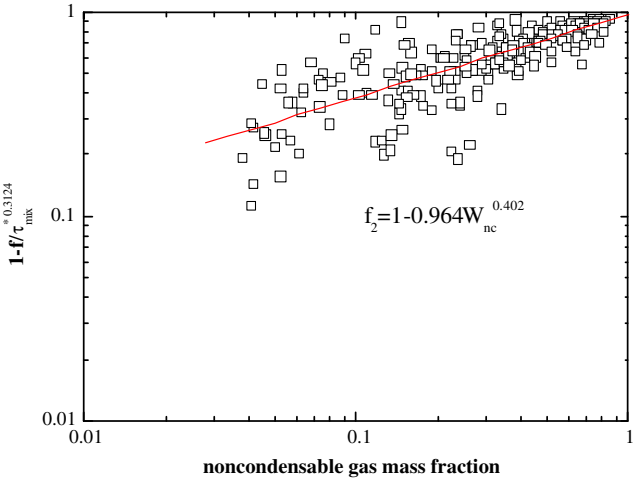

Fig. 6. Factor for the effect of noncondensable gas.

4. Modeling

4.1. Theoretical model

Fig. 7 depicts the problem under investigation schematically. It is assumed that the flow of condensate in the film is laminar, and that the vapor entering the tube is saturated. The inside wall of the tube is at a prescribed temperature T_w, which is lower than the saturation temperature of the vapor. Therefore, condensation takes

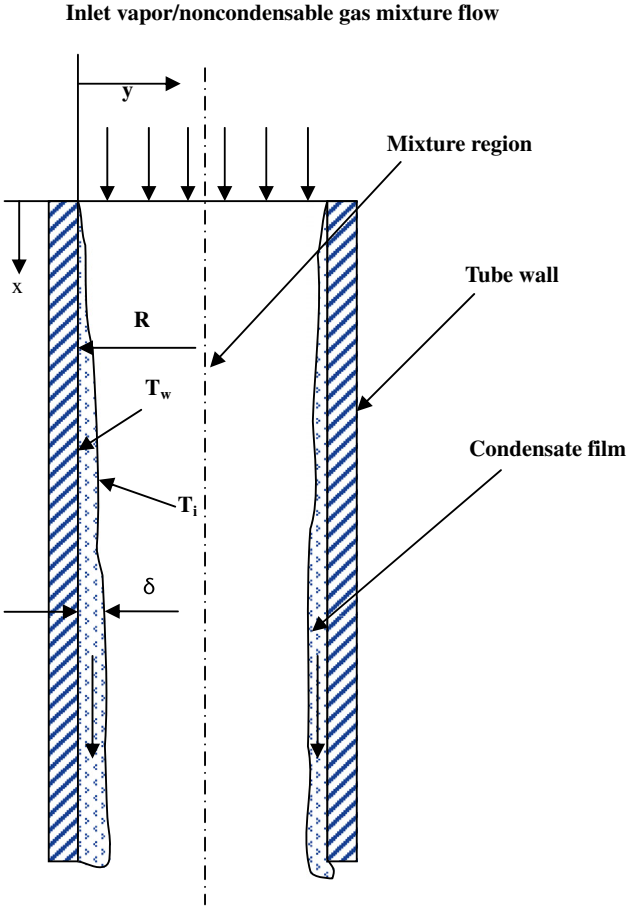

Fig. 7. Schematic view of the physical model.

place on the wall surface. A condensate film forms, of thickness δ, which is a function of the position along the flow direction. The vapor/noncondensable gas mixture has a given inlet bulk temperature T_b, and a corresponding inlet concentration of the noncondensable gas $W_{nc,b}$ at the given pressure. At the liquid/gas interface, the temperature T_i and the noncondensable gas mass fraction $W_{nc,i}$ are unknown and must be determined from the analysis. The analysis of steam condensation in the presence of a noncondensable gas typically involves the heat balance at the liquid/gas interface. However, separate models for the condensate film and vapor/noncondensable gas mixture are linked and solved simultaneously for the heat and mass transfer rates.

The heat transfer through the vapor/noncondensable gas mixture boundary layer consists of the sensible heat transfer and the latent heat transfer given up by the condensing vapor, and it must equal that from the condensate film to the tube wall. Therefore, we get

$$h_f(T_i - T_w) = (h_c + h_s)(T_b - T_i). \tag{10}$$

Then, the total heat transfer coefficient h_{tot} is given by

$$h_{tot} = \left[\frac{1}{h_f} + \frac{1}{h_c + h_s}\right]^{-1}. \tag{11}$$

The condensate film thickness is given by

$$\delta = \frac{1.259\delta_{Nu}^{*4/3}}{[\delta_p(a_1 + a_2x + a_3x^2) + l_i(b_1 + b_2x + b_3x^2 + b_4x^3) + m_i\delta_p(c_1 + c_2x)]^{1/3}}, \tag{12}$$

where a_i, b_i, and c_i are coefficients of polynomial functions in x; and m_i and l_i are functions of the interfacial shear stress. This approximate method proposed by Munoz-Cobo et al. [12] was developed without the need to solve the transcendental equation that depends on the film thickness iteratively. Therefore, it is simple for engineering applications and provides good predictions.

For laminar film, the temperature distribution in the film region is almost linear. Therefore film heat transfer coefficient can be written as

$$h = \frac{k_l}{\delta}. \tag{13}$$

In this study, the heat and mass transfer analogy was used to analyze steam condensation with noncondensable air or nitrogen gas in a vertical tube. Therefore, the sensible and latent heat transfer rates can be calculated simultaneously.

The sensible heat transfer coefficient can be expressed as

$$h_s = Nu_{mix}\frac{k_{mix}}{d_i} \tag{14}$$

and the condensation (or latent) heat transfer coefficient can be defined as

$$h_c = \frac{m''_{cond} i_{fg}}{(T_b - T_i)}. \tag{15}$$

To find m''_{cond}, the mass balance at the interface is calculated to yield the following equation:

$$m''_{cond} = \left[-\rho D\frac{\partial W_v}{\partial y}\right]_i + W_{v,i}(m''_{tot})_i. \tag{16}$$

As the condensate surface is impermeable to the noncondensable gases, Eq. (16) can be simplified as

$$m''_{cond} = \frac{(-\rho D(\partial W_v/\partial y))_i}{1 - W_{v,i}} = h_m\frac{(W_{v,b} - W_{v,i})}{(1 - W_{v,i})}, \tag{17}$$

where h_m is the mass transfer coefficient. Eq. (17) can be recast as

$$Sh_{mix} = \frac{m''_{cond} d}{\rho D}\frac{W_{nc,i}}{(W_{nc,i} - W_{nc,b})}. \tag{18}$$

The modifications necessary to incorporate the condensate film roughness, developing flow, and suction effect on the heat and mass transfer involve modifying the Nusselt and Sherwood numbers, as discussed below.

Film roughness increases the heat transfer from the gas phase by influencing the turbulence pattern close to the interface and disrupting the gaseous laminar sublayer. The method to consider the effect of a wavy surface was considered with the concept of the simple model of Kim and Corradini [17] which applies the mixing length theory presented by Kays and Crawford [18] for a rough surface to the momentum, thermal, and mass concentration boundary layer. The effect of roughness on the heat and mass transfer for flow in a tube was considered using Dipprey and Sabersky's [19] correlation as

$$St = \frac{f_r}{1.0 + \sqrt{f_r}(k_f[Re_g\sqrt{f_r}(\varepsilon_s/d)]^{0.2}Pr^{0.44} - 8.48)}, \tag{19}$$

$$St_{AB} = \frac{f_r}{1.0 + \sqrt{f_r}(k_f[Re_g\sqrt{f_r}(\varepsilon_s/d)]^{0.2}Sc^{0.44} - 8.48)}, \tag{20}$$

where $k_f = 5.19$, $\varepsilon_s/d = e^{(3.0-0.4/\sqrt{f_r})}$, and $f_s = 0.0791Re^{-0.25}$.

Here, the rough wall friction factor f_r is calculated using Whalley and Hewitt [20] correlation for pressures higher than 10^5 Pa as

$$f_r = f_s\left[1 + 24\left(\frac{\rho_l}{\rho_{mix}}\right)^{1/3}\frac{\delta}{d}\right]. \tag{21}$$

In the vapor/noncondensable gas layer, the condensation process leads to thinning of the boundary layer, which is called the suction effect. This means that at the interface, the velocity component normal to the wall is not zero. Kays and Moffat (18) obtained the following correlation for a boundary layer subject to suction experimentally

$$\frac{St}{St_o} = \ln\left(\frac{1 + B_h}{B_h}\right), \tag{22}$$

where $B_h = m''_{cond}/G^\infty St$ is called the suction parameter. This equation can be recast as

$$Nu_x = \left[\exp\left(\frac{m''_{cond}Re_xPr}{G^\infty Nu_{o,x}}\right) - 1\right]^{-1}\left[\frac{G^\infty}{m''_{cond}Re_xPr}\right]^{-1}. \tag{23}$$

Using the analogy between heat and mass transfer, Eq. (23) can be written as

$$Sh_x = \left[\exp\left(\frac{m''_{cond}Re_xSc}{G^\infty Sh_{o,x}}\right) - 1\right]^{-1}\left[\frac{G^\infty}{m''_{cond}Re_xSc}\right]^{-1}. \tag{24}$$

Combining Eqs. (18) and (24), we get m''_{cond} as follows:

$$m''_{cond} = \frac{G^\infty Sh_{o,x}}{Re_xSc}\left[\ln\left\{1 + \frac{Re_xScD\rho(1-\omega)}{G^\infty d}\right\}\right], \tag{25}$$

where ω is the ratio of the noncondensable gas mass fraction in the bulk to that at the liquid/gas interface. As most of the heat transfer takes place in the first part of the condenser tube, it may be important to consider the developing flow effect in the heat and mass transfer model. Therefore, the suggestion of Reynolds et al. [21] is adopted for the thermal entrance zone, and is given by

$$Nu_{o,t} = Nu_o\left[1 + \frac{0.8(1 + 7\times10^4Re^{-3/2})}{x/d}\right] \tag{26}$$

$$Sh_{o,t} = Sh_o\left[1 + \frac{0.8(1 + 7\times10^4Re^{-3/2})}{x/d}\right]. \tag{27}$$

The calculation commences at the tube inlet for which the inlet mixture temperature, inlet steam flow rate, inlet noncondensable gas flow rate, and total pressure are given. Here, the pressure drop through the condenser tube is assumed to be negligible. The inner wall temperature profiles are given as boundary conditions. The heat fluxes through the liquid film and mixture boundary layer are calculated separately with an assumed interface temperature. Iteration is needed to get reasonable heat transfer coefficients of h_f, h_c, and h_s by modifying the interface temperature until the heat fluxes converge within a specified accuracy. The condensing tube is divided into axial control volumes of a specific size of 1 mm. The calculation procedure at each axial location of the tube is explained in Fig. 8.

4.2. Simple models

Simple models using empirical correlations were developed to estimate the condensation heat transfer coefficients of steam/nitrogen or steam/air mixtures easily. These were based on the

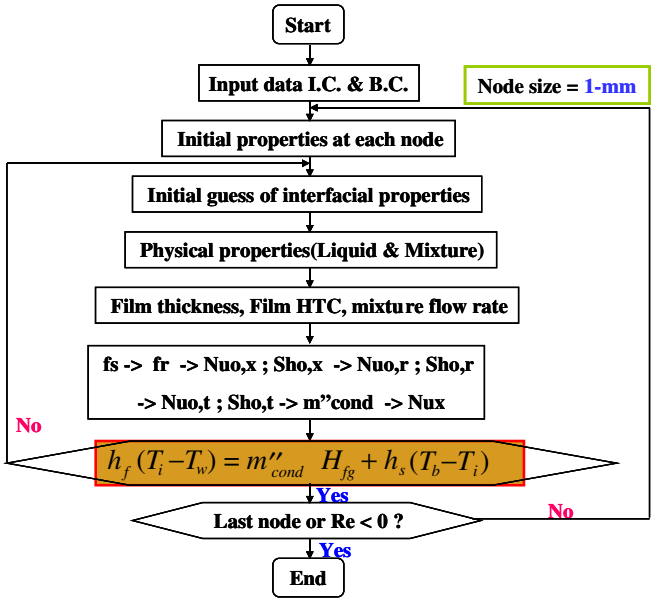

Fig. 8. Calculation procedure.

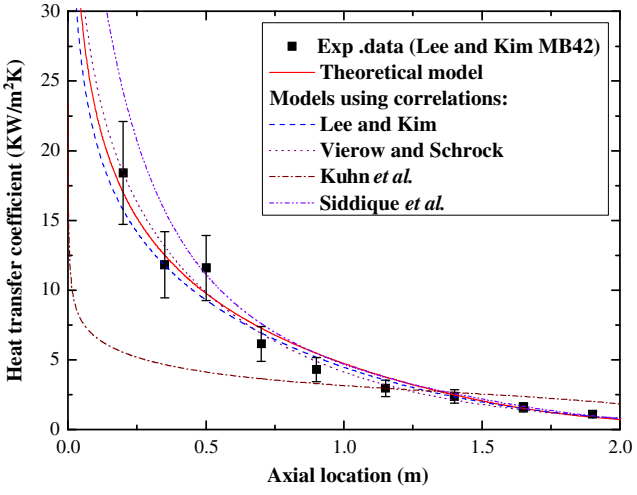

Fig. 9. Comparison of theoretical model and simple models for MB42.

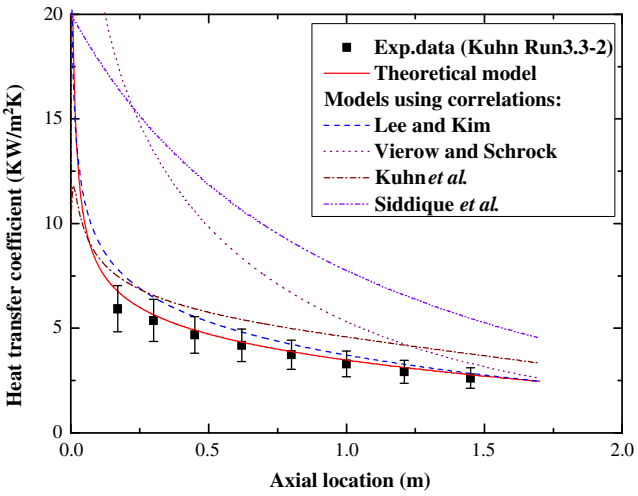

Fig. 10. Comparison of theoretical model and simple models for Run 3.3–2.

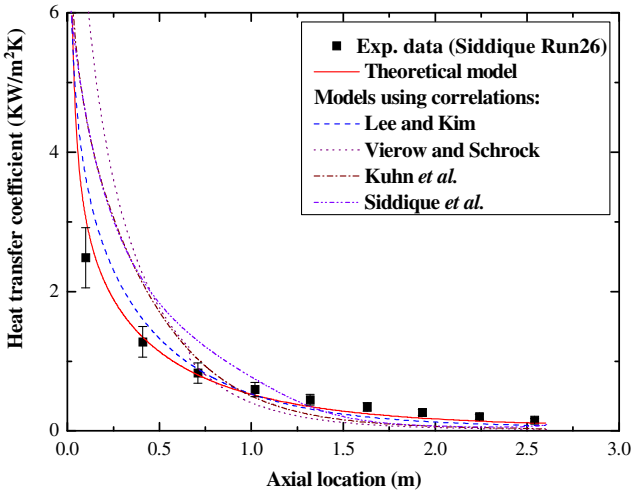

Fig. 11. Comparison of theoretical model and simple models for Run 26.

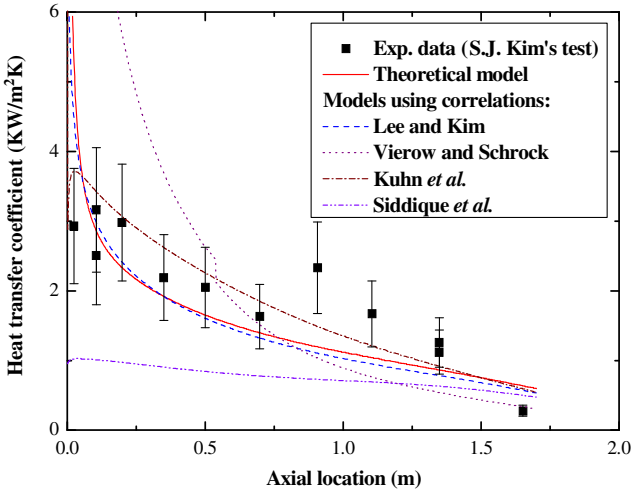

Fig. 12. Comparison of theoretical model and simple models comparison for Kim's sample data.

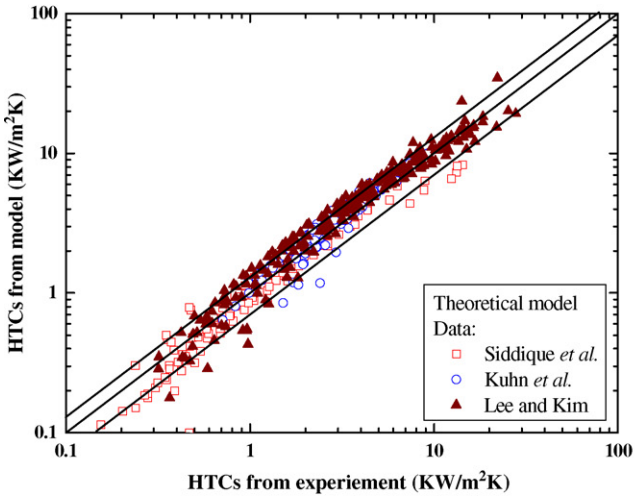

(a) Theoretical model

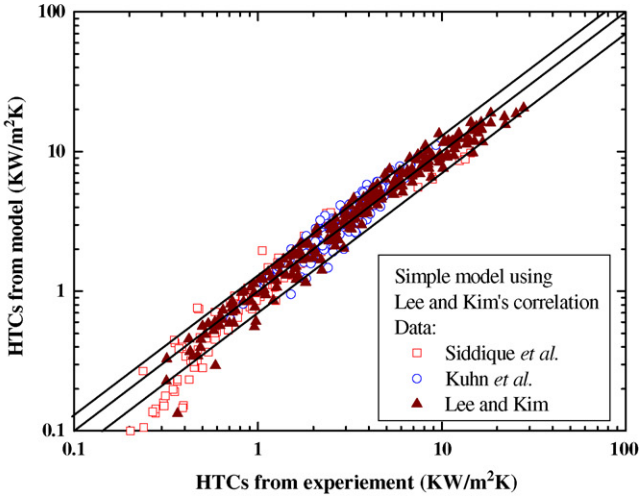

(b) Simple model using Lee and Kim's correlation

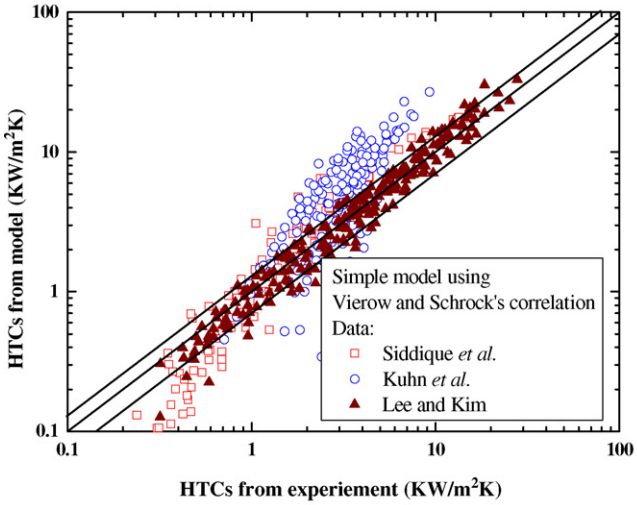

(c) Simple model using Vierow and Schrock's correlation

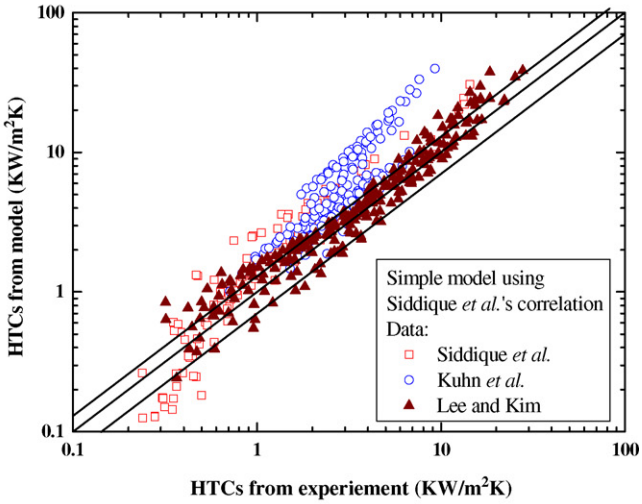

(d) Simple model using Siddique *et al.*'s correlation

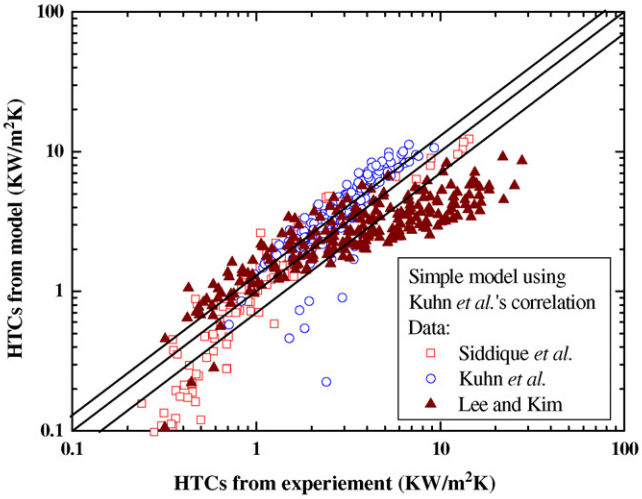

(e) Simple model using Kuhn *et al.*'s correlation

Fig. 13. Comparison of experimental heat transfer coefficients with models.

new correlation (Eq. (9)) and three previous correlations (described below). Even though the previous correlations were developed for a steam/air mixture flow, a comparison with the present data has meaning because the molecular weights of air and nitrogen are very similar.

Vierow and Schrock [1] proposed a correlation that simply expressed the local heat transfer coefficients in the form of a degradation factor, which was a function of the steam/air mixture Reynolds number and bulk local air mass fraction as follows:

$$f = \frac{h_{exp}}{h_{Nu}} = f_1 \cdot f_2 = (1 + aRe_{mix}^{b}) \cdot (1 - cW_{nc}^{d}), \quad (28)$$

where $a = 2.88 \times 10^{-5}$, $b = 1.18$, $c = 10$, and $d = 1.0$ for $W_{nc} < 0.063$; $c = 0.938$ and $d = 0.13$ for $0.063 < W_{nc} < 0.6$; and $c = 1.0$ and $d = 0.22$ for $0.6 < W_{nc}$.

Siddique et al. [2] developed a nondimensional correlation. The governing conservation equations of the vapor/air boundary layer were used as a basis for defining the appropriate nondimensional groups for correlating the data, and the Nusselt number was correlated with the mixture Reynolds number, noncondensable gas mass fraction, Jakob number, and Schmidt number to yield

$$Nu(x) = 6.123 Re_{mix}^{0.223} \left(\frac{W_{nc,w} - W_{nc,b}}{W_{nc,w}} \right)^{1.144} Ja^{-1.253}. \quad (29)$$

Kuhn et al. [4] developed a correlation also using a degradation factor method. A modified form of f_1 was used to evaluate the film heat transfer enhancement due to the effects of interfacial shear and surface waviness. The final form was as follows:

$$f = \frac{h_{exp}}{h_{Nu}} = f_1 \cdot f_2 = f_{1,shear} \cdot f_{1,other} \cdot f_2 = \frac{\delta_{shear}}{\delta_{Nu}} \cdot (1 + a(Re_f/4)) \cdot (1 - bW_{nc}^{c}) \quad (30)$$

where $a = 7.321 \times 10^{-4}$, $b = 2.601$, and $c = 0.708$ for $W_{nc} < 0.1$; and $b = 1.0$ and $c = 0.292$ for $0.1 < W_{nc}$. The condensate film thickness with interfacial shear was obtained from Munoz-Cobo's approximate method (Eq. (12)).

5. Modeling results

Figs. 9–12 show the modeling results for the MB42 (ID = 13 mm, $Re_{mix,in}$ = 33,494, $W_{N_2,in} = 10.2\%$, P = 0.105 MPa), Run 3.3–2 from Kuhn [22] (ID = 47.5 mm, $Re_{mix,in}$ = 37,537, $W_{air,in}$ = 10.2%, P = 0.199 MPa), Run 26 from Siddique [11] (ID = 46 mm, $Re_{mix,in}$ = 15,139, $W_{air,in}$ = 22.4%, P = 0.233 MPa), and the example data from Kim [6] (ID = 46.2 mm, $Re_{mix,in}$ = 42,112, $W_{air,in}$ = 26%, P = 2.9 MPa), respectively. The theoretical model using heat and mass transfer analogy and the simple model based on the new correlation predicted the various sets of experimental data well, and their results were very similar. In particular, Fig. 12 shows that the new correlation can be used to evaluate the condensation heat transfer for a high-pressure steam/noncondensable gas mixture even though it was developed for low-pressure conditions. However, simple models based on the previous empirical correlations exhibited some limitations under various conditions. The model based on the Kuhn et al. [4] correlation underestimated the present data obtained from a small-diameter tube, as shown in Fig. 9. Figs. 10–12 indicate that the model based on the Vierow and Schrock [1] correlation overestimated the data obtained from large-diameter tubes. The model based on the Siddique et al. [2] correlation was not very good for various sets of data, especially at high pressures.

Fig. 13 compares the experimentally estimated heat transfer coefficients with those calculated by the theoretical and simple models, with the standard deviation band of 30%. The simple model based on the Vierow and Schrock [1] correlation was only acceptable for small-diameter condenser tubes, as shown in Fig. 13c. The simple model based on the Siddique et al. [2] correlation predicted the present data well, but it had a narrow range of applicability and its general prediction capabilities were poor for the experimental data obtained by Kuhn et al. [4], as shown in Fig. 13d. The simple model based on the Kuhn et al. [4] correlation had poor prediction capabilities for the most experimental data, as shown in Fig. 13e. However, Fig. 13a and b show that the theoretical model and simple model based on the new correlation not only predicted the present data well, but also the data obtained by other studies. Table 2 summarizes the standard deviation of the models from the experimental data. The theoretical model showed the best prediction ability for the data from large-diameter tubes. The simple model using the new correlation showed the best prediction ability for the data from small-diameter tube, and its abilities for large-diameter tubes were similar with those of theoretical model. Therefore, we propose the new correlation to calculate the steam condensation heat transfer coefficient in the presence of air or nitrogen inside vertical condenser tubes.

Table 2
Comparison of prediction standard deviation by different models

Data set	Number of data points	Standard deviation				
		Theoretical model	Correlations			
			Lee and Kim (%)	Vierow and Schrock (%)	Siddique et al. (%)	Kuhn et al. (%)
Siddique et al.	120	25.0	27.5	61.2	75.6	47.2
Kuhn et al.	158	19.5	20.9	108	129	46.5
Lee and Kim	225	25.8	17.5	22.8	35.5	50.4

6. Conclusion

An experimental study was performed to investigate local condensation heat transfer coefficients in the presence of noncondensable nitrogen gas in a relatively small-diameter vertical tube (ID = 13 mm). The local heat transfer coefficients increased as the inlet steam flow rate increased and the inlet nitrogen mass fraction decreased. The results obtained using pure steam and steam/nitrogen mixtures with low inlet nitrogen gas mass fraction were similar. Therefore, the effects of noncondensable gas on steam condensation were weak in small-diameter condenser tubes because of interfacial shear stress. A new correlation based on dimensionless shear stress and noncondensable gas mass fraction was developed to evaluate the condensation heat transfer coefficient inside a vertical tube with noncondensable gas, irrespective of the condenser tube diameter. We developed a theoretical model using a heat and mass transfer analogy and simple models based on four empirical correlations to analyze steam condensation with noncondensable air or nitrogen gas in a vertical tube. The predictions of the theoretical model and the simple model based on the new correlation showed good agreement with the experimental data obtained under various experimental conditions, including different tube diameters, inlet mixture Reynolds numbers, inlet noncondensable gas fraction, and system pressure, using air or nitrogen as the noncondensable gas.

Acknowledgement

This work was carried out with the support of the SMART R&D Center at KAERI. The authors are grateful for the support.

References

[1] K.M. Vierow, V.E. Schrock, Condensation in a natural circulation loop with noncondensable gases: Part I-Heat Transfer, in: Proceedings of the International Conference on Multiphase Flow, Tsukuba, Japan, 1991, pp. 183–186.

[2] M.S. Siddique, M.W. Golay, M.S. Kazimi, Local heat transfer coefficients for forced-convection condensation of steam in a vertical tube in the presence of a noncondensable gas, Nucl. Technol. 102 (1993) 386–402.

[3] H. Araki, Y. Kataoka, M. Murase, Measurement of condensation heat transfer coefficient inside a vertical tube in the presence of noncondensable gas, J. Nucl. Sci. Technol. 32 (1995) 517–536.

[4] S.Z. Kuhn, V.E. Schrock, P.F. Peterson, An investigation of condensation from steam–gas mixtures flowing downward inside a vertical tube, Nucl. Eng. Des. 177 (1997) 53–69.

[5] H.S. Park, H.C. No, A condensation experiment in the presence of noncondensables in a vertical tube of a passive containment cooling system and its assessment with RELAP5/MOD3.2, Nucl. Technol. 127 (1999) 160–169.

[6] S.J. Kim, Turbulent film condensation of high pressure steam in a vertical tube of passive secondary condensation system, Ph.D. Dissertation, Korea Advanced Institute of Science and Technology, Korea, 2000.

[7] S. Oh, S.T. Revankar, Effect of noncondensable gas in a vertical tube condenser, Nucl. Eng. Des. 235 (2005) 1699–1712.

[8] A.P. Colburn, O.A. Hougen, Design of cooler condensers for mixture of vapors with non-condensable gases, Ind. Eng. Chem. 26 (1934) 1178–1182.

[9] C.-Y. Wang, C.-J. Tu, Effects of non-condensable gas on laminar film condensation in a vertical tube, Int. J. Heat Mass Transfer 31 (1988) 2339–2345.

[10] T. Kageyama, P.F. Peterson, V.E. Schrock, Diffusion layer modeling for condensation in vertical tubes with noncondensable gases, Nucl. Eng. Des. 141 (1993) 289–302.

[11] M.S. Siddique, The effects of noncondensable gases on steam condensation under forced convection conditions, Ph.D. Dissertation, Massachusetts Institute of Technology, Cambridge, MA, 1992.

[12] J.L. Munoz-Cobo, L. Herranz, J. Sancho, I. Tkachenko, G. Verdu, Turbulent vapor condensation with noncondensable gases in vertical tubes, Int. J. Heat Mass Transfer 39 (1996) 3249–3260.

[13] H.C. No, H.S. Park, Non-iterative condensation modeling for steam condensation with non-condensable gas in a vertical tube, Int. J. Heat Mass Transfer 45 (2002) 845–854.

[14] N.K. Maheshwari, D. Saha, R.K. Sinha, M. Aritomi, Investigation on condensation in presence of a noncondensable gas for a wide range of Reynolds number, Nucl. Eng. Des. 227 (2004) 219–238.

[15] S. Oh, S.T. Revankar, Experimental and theoretical investigation of film condensation with noncondensable gas, Int. J. Heat Mass Transfer 49 (2006) 2523–2534.

[16] P.F. Peterson, V.E. Schrock, S.Z. Kuhn, Recent experiments for laminar and turbulent film heat transfer in vertical tubes, Nucl. Eng. Des. 175 (1997) 157–166.

[17] M.H. Kim, M.L. Corradini, Modeling of condensation heat transfer in a reactor containment, Nucl. Eng. Des. 118 (1990) 193–212.

[18] W.M. Kays, M.E. Crawford, Convective Heat and Mass Transfer, MaGraw-Hill, 1980.

[19] D.F. Dipprey, R.H. Sabersky, Heat and momentum transfer in smooth and rough tubes at various Prandtl numbers, Int. J. Heat Mass Transfer 6 (1963) 329–353.

[20] P.B. Whalley, G.F. Hewitt, The correlation of liquid entrainment fraction and entrainment rate in annular two phase flow, AERE-R-878 (1978).

[21] H.C. Reynolds, T.B. Swearingen, D.M. McEligot, Thermal entry for low Reynolds number turbulent flow, J. Basis Eng. 91 (1969) 87–94.

[22] S.Z. Kuhn, Investigation of heat transfer from condensing steam–gas mixtures and turbulent films flowing downward inside a vertical tube, Ph.D. Dissertation, University of California, Berkeley, CA, 1995.